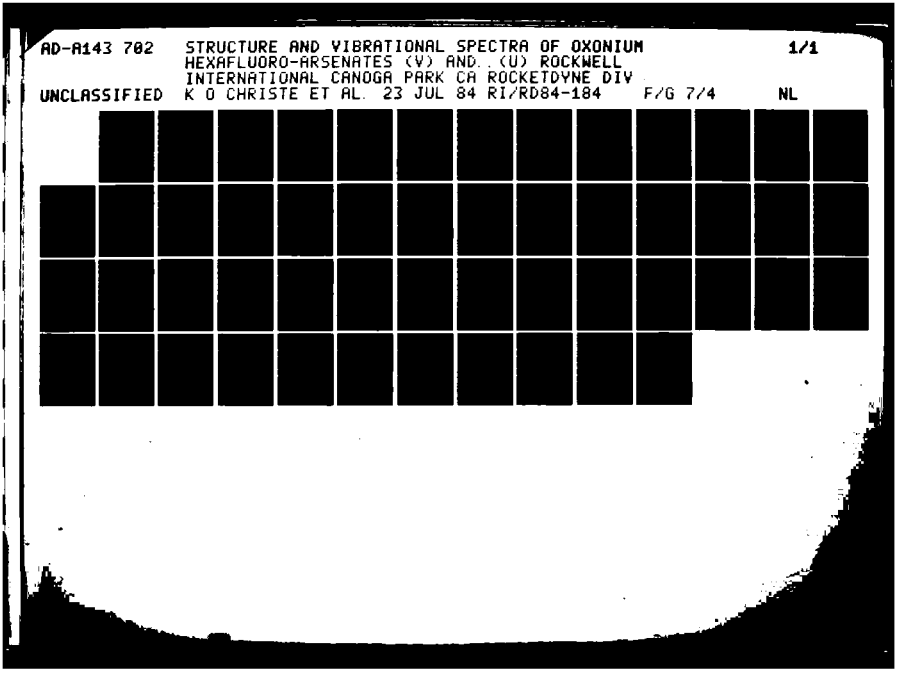
AD-A143 702 STRUCTURE AND VIBRATIONAL SPECTRA OF OXONIUM HEXAFLUORO-ARSENATES (V) AND.. (U) ROCKWELL INTERNATIONAL CANOGA PARK CA ROCKETDYNE DIV
1/1
UNCLASSIFIED K O CHRISTE ET AL. 23 JUL 84 RI/RD84-184 F/G 7/4
NL

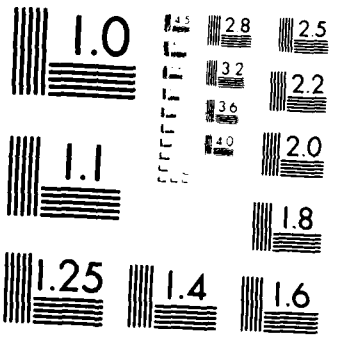

Unclassified

SECURITY CLASSIFICATION OF THIS PAGE (When Data Entered)

(12)

REPORT DOCUMENTATION PAGE		READ INSTRUCTIONS BEFORE COMPLETING FORM
1. REPORT NUMBER Technical Report 2	2. GOVT ACCESSION NO.	3. RECIPIENT'S CATALOG NUMBER
4. TITLE (and Subtitle) Structure and Vibrational Spectra of Oxonium Hexafluoro-Arsenates (V) and-Antimonates (V)		5. TYPE OF REPORT & PERIOD COVERED Technical Report 6. PERFORMING ORG. REPORT NUMBER RI/RD84-184
7. AUTHOR(s) Karl O. Christe,*[1] P. Charpin,[2] E. Soulie,[2] R. Bougon,[2] J. Fawcett,[3] and D. R. Russell[3]		8. CONTRACT OR GRANT NUMBER(s) N00014- 83-C-0531
PERFORMING ORGANIZATION NAME AND ADDRESS Rocketdyne, 6633 Canoga Avenue, Canoga Park, CA 91304 Centre d'Etudes Nucleaires de Saclay, 91191 Gif-sur-Yvette Cedex, France (Cont. Pg 2)		10. PROGRAM ELEMENT PROJECT, TASK AREA & WORK UNIT NUMBERS NR 053-840
CONTROLLING OFFICE NAME AND ADDRESS Office of Naval Research Department of the Navy Arlington, Virginia 22217		12. REPORT DATE July 23, 1984 13. NUMBER OF PAGES 11
MONITORING AGENCY NAME & ADDRESS(if different from Controlling Office)		15. SECURITY CLASS. (of this report) Unclassified 15a. DECLASSIFICATION DOWNGRADING SCHEDULE

AD-A143 702

DISTRIBUTION STATEMENT (of this Report)

Approved for public release; distribution unlimited

DTIC FILE COPY

DTIC ELECTE JUL 26 1984 B

17. DISTRIBUTION STATEMENT (of the abstract entered in Block 20, if different from Report)

18. SUPPLEMENTARY NOTES

To be published in Inorganic Chemistry

19. KEY WORDS (Continue on reverse side if necessary and identify by block number)

Oxonium Hexafluoroarsenate (V)
Oxonium Hexafluoroantimonate (V)
Structure
Vibrational Spectra
Force field
X-ray diffraction
Neutron diffraction
DSC data
Phase transitions

20. ABSTRACT (Continue on reverse side if necessary and identify by block number)

The salts $OD_3^+AsF_6^-$, $OD_3^+SbF_6^-$ and partially deuterated $OH_3^+SbF_6^-$ were prepared and characterized by X-ray and neutron diffraction techniques, DSC measurements, and vibrational spectroscopy. At room temeprature, $OH_3^+AsF_6^-$ exists in a plastic phase where ions, centered on the atomic positions of the NaCl structure, are in motion or oscillation. No valuable information on atomic distances or angles in

DD FORM 1 JAN 73 1473 EDITION OF 1 NOV 65 IS OBSOLETE

Unclassified

SECURITY CLASSIFICATION OF THIS PAGE (When Data Entered)

9. (Continued)

Department of Chemistry, University of Leicester, Leicester LEI 7RH, u.K.

20. (Continued)

$OH_3^+AsF_6^-$ could be obtained due to these dynamic structural disorder problems. For $OH_3^+SbF_6^-$ the phase transition from an ordered to a disordered phase was shown to occur above room temperature. The room temperature phase can be described by an ordered hydrogen bonded model based on a CsCl type structure. Vibrational spectra were recorded for these oxonium salts and confirm the presence of the different phases and phase transitions. Improved assignments are given for the OH_3^+ and OD_3^+ cations, and the OH...FM bridge stretching mode and some of the bands characteristic for OD_2H^+ and ODH_2^+ were identified. A modified valence force field was calculated for OH_3^+ which is in good agreement with the known general valence force field of isoelectronic NH_3 and values obtained by ab initio calculations. From the OH...FM stretching mode, the hydrogen bridge bond strength was found to be 1.77 kcal mol^{-1}.

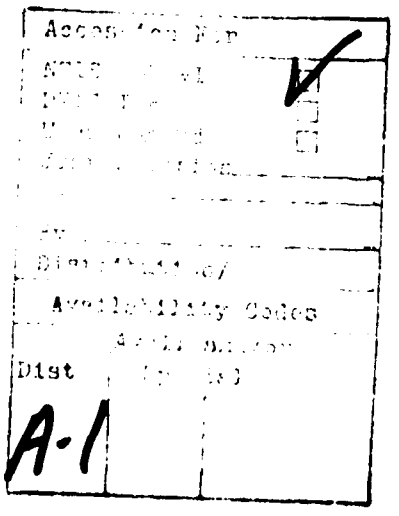

OFFICE OF NAVAL RESEARCH

Contract N00014-83-C-0531

Task No. NR 053-840

TECHNICAL REPORT NO. 2

Structure and Vibrational Spectra of Oxonium Hexafluoro-Arsenates (V) and-Antimonates (V)

by

K. O. Christe,*[1] P. Charpin,[2] E. Soulie,[2] R. Bougon,[2] J. Fawcett,[3] and D. R. Russell[3]

Rocketdyne
A Division of Rockwell International
Canoga Park, CA 91304

Centre d'Etudes Nucleaires
de Saclay, 91191 Gif-sur-Yvette
Cedex, France,

Department of Chemistry
University of Leicester,
Leicester LEI 7RH, U.K.

July 23, 1984

Prepared for publication in Inorganic Chemistry

Contribution from Rocketdyne, A Division of
Rockwell International, Canoga Park, California 91304
the Centre d'Etudes Nucleaires de Saclay, 91191 Gif-sur-Yvette Cedex,
France, and the Department of Chemistry, University of Leicester,
Leicester LEI 7RH, U.K.

Structure and Vibrational Spectra of Oxonium Hexafluoro-Arsenates (V) and-Antimonates (V)

K. O. Christe,*[1] P. Charpin,[2] E. Soulie,[2] R. Bougon,[2] J. Fawcett,[3]
and D. R. Russell[3]

Abstract

The salts $OD_3^+AsF_6^-$, $OD_3^+SbF_6^-$ and partially deuterated $OH_3^+SbF_6^-$ were prepared and characterized by X-ray and neutron diffraction techniques, DSC measurements, and vibrational spectroscopy. At room temperature, $OH_3^+AsF_6^-$ exists in a plastic phase where ions, centered on the atomic positions of the NaCl structure, are in motion or oscillation. No valuable information on atomic distances or angles in $OH_3^+AsF_6^-$ could be obtained due to these dynamic structural disorder problems. For $OH_3^+SbF_6^-$ the phase transition from an ordered to a disordered phase was shown to occur above room temperature. The room temperature phase can be described by an ordered hydrogen bonded model based on a CsCl type structure. Vibrational spectra were recorded for these oxonium salts and confirm the presence of the different phases and phase transitions. Improved assignments are given for the OH_3^+ and OD_3^+ cations, and the OH...FM bridge stretching mode and some of the bands characteristic for OD_2H^+ and ODH_2^+ were identified. A modified valence force field was calculated for OH_3^+ which is in good agreement with the known general valence force field of isoelectronic NH_3 and values obtained by ab initio calculations. From the OH...FM stretching mode, the hydrogen bridge bond strength was found to be 1.77 kcal mol^{-1}.

Introduction

Although the existence of oxonium salts at low temperature had been well known for many years, the synthesis of surprisingly stable OH_3^+ salts containing the AsF_6^- and SbF_6^- anions has been reported[4] only in 1975. Since then numerous papers have been published on other OH_3^+ salts containing complex fluoro anions, such as UF_6^-,[5] BiF_6^-,[6] IrF_6^-, PtF_6^-, RuF_6^-,[7,8] TiF_5^-,[9] or BF_4^-.[10] In these oxonium salts the cations and anions are strongly hydrogen bonded, as shown by the short O-F distances of 2.51 to 2.61Å found by X-ray diffraction studies.[9,10] Since the nature of these hydrogen bridges is strongly temperature dependent, these oxonium salts show phase transitions and present interesting structural problems. In this paper we report unpublished results accumulated during the past eight years in our laboratories for these oxonium salts.

Experimental Section

Materials and Apparatus. Volatile materials used in this work were manipulated in a well-passivated (with ClF_3 and HF or DF) Monel-Teflon FEP vacuum system.[11] Nonvolatile materials were handled in the dry nitrogen atmosphere of a glove box. Hydrogen fluoride (The Matheson Co.) was dried by storage over BiF_5.[6] SbF_5 and AsF_5 (Ozark Mahoning Co.) were purified by distillation and fractional condensation, respectively, and DF (Ozark Mahoning Co.) and D_2O (99.6%, Volk) were used as received. Literature methods were used for the preparation of O_2AsF_6[12] and OH_3SbF_6 and OH_3AsF_6.[4]

Infrared spectra were recorded on a Perkin-Elmer Model 283 spectrometer, which was calibrated by comparison with standard gas calibration points.[13,14] Spectra of solids were obtained by using dry powders pressed between AgCl or AgBr windows in an Econo press (Barnes Engineering Co.). For low-temperature spectra, the pressed silver halide disks were placed in a copper block cooled to -196°C with liquid N_2 and mounted in an evacuated 10 cm path length cell equipped with CsI windows.

Raman spectra were recorded on a Cary Model 83 spectrophotometer using the 4880-Å exciting line and a Claassen filter[15] for the elimination of plasma lines. Sealed quartz tubes were used as sample containers in the transverse-viewing, transverse-excitation technique. The low-temperature spectra were recorded using a previously described[16] device.

A Perkin-Elmer differential scanning calorimeter, Model DSC-1B, equipped with a liquid N_2 cooled low-temperature assembly, was used to measure phase transitions above -90°C. The samples were crimp sealed in aluminum pans, and a heating rate of 5°/min in N_2 was used. The instrument was calibrated with the known mp of n-octane, water, and indium.

The neutron powder diffraction patterns of $OH_3^+AsF_6^-$, $OD_3^+AsF_6^-$, and $O_2^+AsF_6^-$ were measured at Saclay using the research reactor EL3 with λ = 1.140Å for 2θ ranging from 6 to 44°. The data for $OD_3^+SbF_6^-$ were recorded at ILL Grenoble with λ = 1.2778Å for 2θ ranging from 12 to 92° with 400 measured values of intensity separated by 0.10°.

The X-ray powder diffraction patterns were obtained from samples sealed in 0.3mm Lindemann capillaries with a 114.6mm diameter Philips camera using Ni-filtered Cu Kα radiation. Low-temperature diagrams were measured using a jet of cold N_2 to cool the sample and a Meric MV3000 regulator.

The single crystal of $OH_3^+SbF_6^-$ was isolated as a side product from the reaction of MoF_4O and SbF_5 in a thin walled Teflon FEP reactor with H_2O slowly diffusing through the reactor wall.

Preparation of $OD_3^+AsF_6^-$. A sample of D_2O (987.5mg, 49.30mmol) was syringed in the drybox into a 3/4 inch Teflon FEP ampule equipped with a Teflon coated magnetic stirring bar and a stainless steel valve. The ampule was connected to a Monel-Teflon vacuum line, cooled to -196°C, evacuated, and DF (10g) was added. The mixture was homogenized at room temperature, and AsF_5 (57.7mmol) was added at -196°C. The mixture was warmed to -78°C and then to ambient

temperature for 1 hr with agitation. All material volatile at ambient temperature was pumped off for 2 hr, leaving behind a white solid residue (10.408g, weight calcd for 49.30mmol of $OD_3^+AsF_6^-$ 10.402g) identified by IR spectroscopy as mainly $OD_3^+AsF_6^-$ containing a small amount (less than 1%) of $OD_2H^+AsF_6^-$ as impurity.

Preparation of $OD_3^+SbF_6^-$. Antimony pentafluoride (18.448g, 85.11mmol) was added in the drybox to a 3/4 inch Teflon FEP ampule equipped with a Teflon coated magnetic stirring bar and a stainless steel valve. The ampule was connected to the vacuum line, cooled to -78°C, evacuated and DF (23.1g) was added. The mixture was homogenized at room temperature. The ampule was cooled inside the drybox to -196°C, and D_2O (1.6951g, 84.63mmol) was added with a syringe. The mixture was agitated for several hours at 25°C, and all material volatile at 45°C was pumped off for 14 hr. The white solid residue (21.987g, weight calcd for 84.63mmol of $OD_3^+SbF_6^-$ 21.813g) was identified by spectroscopic methods as mainly $OD_3^+SbF_6^-$ containing a small amount (less than 1%) of $OD_2H^+SbF_6^-$.

Preparation of Partially Deuterated $OH_3^+SbF_6^-$. A sample of $OH_3^+SbF_6^-$ (2.0016g, 7.857mmol) was dissolved in liquid DF (2.012g, 95.81mmol) in a Teflon ampule for 1 hr. All volatile material was pumped off at 45°C for 3 hr leaving behind a white solid residue (2.020g, weight calcd for 7.857mmol of $OD_3^+SbF_6^-$ 2.0252g) which based on its vibrational spectra showed about equimolar amounts of OD_3^+ and OD_2H^+, and smaller amounts of $ODH_2^+SbF_6^-$ (calcd statistical product distribution for 19.74%H and 80.26%D: OD_3^+ 51.68, OD_2H^+ 38.16, ODH_2^+ 9.33, and OH_3^+ 0.77 mol%).

Results and Discussion

Syntheses and Properties of Deuterated Oxonium Salts. The OD_3^+ salts were prepared by the same method as previously reported[4] for the corresponding OH_3^+ salts, except for replacing H_2O and HF by D_2O and DF, respectively.

$$D_2O + DF + MF_5 \xrightarrow{DF} OD_3^+MF_6^- \quad (M=As,Sb)$$

The yields are quantitative and the samples were almost completely deuterated. The small amounts of OD_2H^+ observed in the infrared spectra and to a lesser degree in the Raman spectra of the products (see below), are attributed to small amounts (0.6%) of H_2O in the D_2O starting material and to exchange with traces of moisture during the preparation of the IR samples. A partially deuterated sample of $OH_3^+SbF_6^-$ was prepared by treating solid $OH_3^+SbF_6^-$ with an excess of DF.

$$OH_3^+SbF_6^- + nDF \longrightarrow OH_{3-n}D_n^+SbF_6^- + nHF$$

The exchange appeared to be fast, and the product exhibited the correct statistical OD_3^+, OD_2H^+, ODH_2^+, OH_3^+ distribution based on the H:D ratio of the starting materials. As expected, the physical properties of the deuterated oxonium salts were practically identical to those[4] of the corresponding OH_3^+ salts.

DSC Data. Since the neutron and X-ray diffraction data suggested (see below) that at room temperature OH_3SbF_6 is ordered whereas OH_3AsF_6 exists in a plastic phase, low-temperature DSC data were recorded to locate the corresponding phase changes for each compound.

The OD_3AsF_6 salt exhibited on warm up from -90°C a large endothermic phase change at 2.5° which was shown to be reversible, occurring at -7.5° on cooling. For OH_3AsF_6 this phase change was observed at practically the same temperatures. No other endotherms or exotherms were observed between -90°C and the onset of irreversible decomposition. The observed phase change temperatures are in excellent agreement with those found by low-temperature Raman spectroscopy (see below).

For OH_3SbF_6 three small endotherms at 20, 49, and 81°C and a large endothermic phase change at 100°C were observed on warming. All of these were reversible occurring at 19, 42, 77 and 96°C, respectively, on cooling. For OD_3SbF_6 the

corresponding changes were observed at 20, 48, 82, and 100°C on warming and 20, 43, 74, and 76°C on cooling. Again no other heat effects were observed in this temperature range. The temperature differences observed for phase changes between the heating and cooling data is attributed to hysteresis which normally is a problem in salts of this type.[17] The smaller heat effects observed for OH_3SbF_6 below the major order-disorder phase transition may be attributed to damping of rotational motions of the ions, similar to those found for O_2AsF_6.[17]

For OH_3BiF_6 no phase transitions were observed between -90°C and the onset of decomposition.

Structural Studies

OH_3AsF_6. As previously reported,[4] this compound is cubic at room temperature, and a cell parameter of 8.043(8)Å was found in this study from X-ray powder data. It exhibits only one phase transition at -2±5°C (based on DSC and Raman data) in the temperature range from -90°C to its decomposition point. The X-ray powder pattern at -153°C is given in Table 1 and indicates a lowering of the symmetry in agreement with the low-temperature vibrational spectra (see below). Attempts to index the pattern were unsuccessful.

It is interesting to compare the X-ray powder diffraction patterns of OH_3AsF_6 and O_2AsF_6. Whereas their room temperature patterns[4,12,18] and cell parameters are for practical purposes identical, their low-temperature patterns (Table 1 and ref. 19) are very distinct due to different ion motion freezing. Since OH_3^+, OD_3^+, and O_2^+ are weak X-ray scatterers, but contribute strongly to the neutron scattering, neutron diffraction powder patterns were also recorded at room temperature for their AsF_6^- salts (see Table II). As expected, the cell dimensions were for practical purposes identical, but the observed relative intensities were very different.

Attempts were made to obtain structural information from the room-temperature neutron diffraction powder patterns of OH_3AsF_6 and OD_3AsF_6. It was shown that the unit cell is indeed face-centered cubic and that an alternate solution,[4] a primitive cubic $CsPF_6$ structure, can be ruled out for both compounds. The number of observed peaks is rather small, but the respective intensities due to the substitution of hydrogen by deuterium (scattering lengths $b_H = -0.374$, $b_D = 0.667$) are very different (Table II). The rapid vanishing of intensities at large diffraction angles and the presence of a bump in the background level implying a short distance order, are characteristic of plastic phases with ions in motion. The only models which could be tested to describe such a motion have been tried successively.

The first one is a disordered model with statistical occupancy factors for fluorine atoms and hydrogen atoms in the Fm3 symmetry group. This corresponds to four equivalent positions of the octahedra around the fourfold axes, and to eight positions for the OH_3^+ ion. Using the intensities observed for OH_3AsF_6, the solution refines to R = 0.047, but is not considered acceptable because the resulting distances As-F = 1.58Å and O-H = 0.82Å are too short when compared to As-F = 1.719(3)Å in $KAsF_6$[20] and O-H = 1.011(8)Å in $OH_3^+p\text{-}CH_3C_6H_4SO_3^-$.[21]

The second one is a rotating model which places As at the 000 position connected to fluorines by a complex term

$$b_{As} + 6b_F \frac{\sin x}{x} \quad \text{with } x = 4\pi r_F \sin\theta/\lambda$$

and O at the 1/2 1/2 1/2 position connected to H atoms by

$$b_O + 3b_H \frac{\sin x}{x} \quad \text{with } x = 4\pi r_H \sin\theta/\lambda$$

where b_{As}, b_F, b_O and b_H are the scattering lengths of As, F, O, and H, respectively. The As-F distance, r_F, and the O-H distance, r_H, are the only unknowns with the scale factor of the structure.[22] The best results

(R = 0.059) are obtained with the combination As-F = 1.59Å and O-H = 0.81Å, not so different indeed from the first model.

For OD_3AsF_6, the second model gives more plausible distances, As-F = 1.65Å and O-D = 1.01Å with R = 0.054, if the intensity of the 200 reflexion is arbitrarily lowered by 20% assuming the excessive intensity being due to preferential orientation.

Based on the short distances found for OH_3AsF_6, we can consider that the real structure is probably not properly accounted for by either one of the models, due to the motion of the ions which is not correctly simulated as for other plastic phases.

OH_3SbF_6. Based on the DSC data (see above) the transition from an ordered to a disordered phase occurs at 88±12°C. The existence of an ordered phase at room temperature for OH_3SbF_6 and its deuterated analogues was confirmed by the diffraction studies. The X-ray powder diffraction pattern, which originally had been read backwards due to very intense back reflections and indexed incorrectly as tetragonal,[4] is listed in Table III. By analogy with a large class of other MF_6^- compounds, such as O_2PtF_6[23] and O_2SbF_6,[24] the OH_3SbF_6 pattern can be indexed for a cubic unit cell with a = 10.143(3)Å (CEN data) or 10.090Å (Rocketdyne data). The cell dimensions were confirmed by a single crystal X-ray study at Leicester (see below) which resulted in a = 10.130(8)Å. Although all of the observed X-ray reflections obey the conditions (h+k+l=2n and 0kl where k,l=2n) for space group Ia3, the neutron diffraction data (see below) suggest a lower symmetry subgroup, such as $I2_13$. In the following paragraphs the results obtained for the ordered cubic, room temperature phase of OH_3SbF_6 are discussed in more detail.

Single Crystal X-ray Study. The OH_3SbF_6 single crystal had the approximate dimensions 0.46 x 0.35 x 0.22mm and was sealed in a Pyrex capillary. Preliminary cell dimensions were obtained from Weissenberg and precession

photographs. The final value for the unit cell parameter was determined from the optimized counter angles for zero layer reflections on a Stoe Weissenberg diffractometer. The data were collected for layers 0kl to 6kl of the aligned pseudotetragonal cell, using the Stoe Stadi-2 diffractometer, in the four quadrants h ± k ± l and an ω-scan technique with graphite monochromated Mo Kα radiation. The intensities of reflections with $0.086 \leq \sin\theta/\lambda \leq 0.702 \text{Å}^{-1}$ were collected, and a total of 719 reflections obtained with $I/\sigma I \geq 3$. Check reflections were monitored during the data collection of each layer and no deterioration of the crystal was indicated. Lorentz and polarisation corrections were made to the data set.

The program system SHELX[25] was used to solve the structure. Neutral scattering factors were used with anomalous dispersion coefficients. Three cycles of least squares refinement with antimony at $(\frac{1}{2}, \frac{1}{2}, \frac{1}{2})$ in the space group Ia3 gave an R factor of 0.27. The Fourier difference map located a 9 $e\text{Å}^{-3}$ peak, assumed to be oxygen, on the position $(\frac{1}{4}, \frac{1}{4}, \frac{1}{4})$, with two sets of possible fluorine octahedra each at 1.90Å from Sb. Three cyles of refinement with the oxygen atom included reduced the R factor to 0.22. The inclusion of either of the sets of F atoms about Sb, with all atoms refining isotropically, resulted in a reduced R factor of 0.13; however, the refinment cycles moved the F atoms to > 2.0Å from Sb. The inclusion of fluorine atoms also resulted in a more complex difference Fourier map, with several peaks ≈3 $e\text{Å}^{-3}$ remaining. The alternate fluorine atom positions indicated were refined in partially occupied sites initially adjusting the site occupation factors and then their temperature factors. The resultant R factor of 0.12 was not significantly less than with either ordered structure; one of the partial fluorine atoms refined to a position 2.2Å from Sb, and further possible fluorine sites appeared in the Fourier map. Refinement of various models with either ordered fluorine atoms or disordered atoms constrained to be 1.86(3)Å from antimony, did not improve the R factor or the residual Fourier map. Accordingly, the F atom parameters given in Table IV represent an ordered solution in Ia3, the actual F atom chosen was that which remained at the expected distance from antimony during the various trial refinements. This

represents an incomplete solution, as there are residual peaks at Sb-F distances in the final Fourier difference map. This is reflected in the structure factors, where agreement between |Fo| and |Fc| is good for even, even, even reflections with dominant contribution by the antimony and oxygen atoms but poor for odd, odd, even reflections which are dependent only upon the fluorine (and hydrogen) atom parameters. Final residual indices for 155 unique reflections is R = 0.119, R_w = 0.131.

Neutron Powder Diffraction Study. For OD_3SbF_6 46 reflexions were observed (see Figure 1) out of which 4 could not be indexed on the basis of the cubic cell and are attributed to an unidentified impurity (mainly lines at 3.269, 2.235 and 2.225Å). The list of observed reflexions is given in Table V in comparison with X-ray data. The cell parameter is 10.116(6)Å.

The Rietveld program for profile refinement[26] was used to solve the structure. The first refinement was attempted in the Ia3 space group starting from the X-ray values for Sb, O and F and adding approximate values for D with the OD_3^+ ion being disordered on two equivalent positions (occupancy factor = ½ of general positions xyz). The system refined to R = 0.135 with the following parameters:

Atom	x	y	z	B (Å^2)
Sb	0.5	0.5	0.5	0.94(25)
O	0.25	0.25	0.25	4.87(41)
F	0.441(6)	0.604(6)	0.641(7)	2.88(13)
D	0.300(1)	0.317(1)	0.204(1)	2.98(27)

The y and z coordinates of the fluorine atom have been permuted, probably due to the choice of the coordinates of deuterium. The atomic distances and angles

are then

Sb-F	1.87Å	
O-F	2.67Å	
O-D	0.96Å	
D-D	1.56Å	DOD: 108°

which compare relatively well with the X-ray values of Table IV. At this stage, our attention was drawn to the presence of a weak but well isolated line at an angle θ high enough not to be attributed to the impurity. This line corresponded to a 730 reflexion, a forbidden reflexion in the space group Ia3 (hko, h, k, = 2n). In view of a similar observation for the cubic phase of $KSbF_6$(II) (in this case the 310 reflexion),[27] the trouble with locating the fluorine atoms by difference X-ray syntheses, and mainly the incompatibility of the group Ia3 with the observed Raman and IR spectra (see below), we considered the possibility of an ordered structure in a subgroup of the Ia3 space group, first the noncentrosymmetric $I2_13$ space group (No. 199).

Since the symmetry center does not exist anymore, the local symmetry of the Sb and O atoms is then only a threefold axis. The structure has to be described with two sets of fluorine atoms F_1 and F_2, and the oxonium ion is ordered with a full occupation of deuterium atoms on the general positions. The Sb and O atoms are also allowed to move along the threefold axes from their ideal positions (000, 1/2, 1/2, 1/2).

This hypothesis was tested and led to a better R factor (0.106) with the following parameters:

Atom	x	y	z	B(Å^2)
Sb	-0.012(1)	-0.012(1)	-0.012(1)	0.13(0.38)
O	0.238(3)	0.238(3)	0.238(3)	3.50(0.75)
F1	0.044(1)	-0.118(1)	-0.143(2)	1.26(0.42)
F2	-0.75(2)	0.091(1)	0.137(2)	1.89(0.45)
D	0.199(2)	0.184(1)	0.299(1)	3.40(0.30)

Figure 1 gives the resulting profile of observed and calculated neutron diffraction diagrams and shows satisfactory agreement.

The Sb and O atoms are displaced from their ideal positions by 0.21Å, and the environment of the Sb atom has 3 F_1 atoms at 1.80Å and 3F_2 atoms at 1.94Å, which seems to be compatible with the Raman and IR spectra.

The F_2 atoms are closer to the oxygen atom of the oxonium group than the F_1 atoms with F_2-O = 2.60Å and F_1-O = 2.79Å. The F_2-O distance is within the correct range for a strong OD...F hydrogen bridge bond (2.51-2.56Å in OH_3TiF_5[9] and 2.58-2.61Å in OH_3BF_4[10]).

The deuterium atoms are located at 0.91Å from the oxygen atom, (with a D-D distance of 1.54Å and a DOD angle of 116°) on the line O-F_2 (OD + DF_2 = 0.91 + 1.69 = 2.60Å). This confirms, in the precision of our results, the quasi linearity of the O-D...F bond in this compound. The geometry of the OD_3^+ cation itself is a flat pyramid with C_3 symmetry. The oxygen atom lies 0.18Å out of the plane of the 3 deuterium atoms.

Figure 2 illustrates the environment around the oxonium ion, with the F_2 atoms being differentiated from the F_1 atoms by traces of the ellipses. The two SbF_6^- octahedra fully represented are approximately located at 000 and 1/2 1/2 1/2 along the [111] direction and bring the environment to an icosahedron. The distinction between F_1 and F_2 implies a small displacement of the fluorine atoms from their average positions obtained in the Ia3 space group (F-F_1 or F-F_2 distances are about 0.20Å) but the angular distortion of the octahedron is small, one side being flattened and the other one being elongated. To obtain a refinement in the $I2_13$ symmetry group, we had to allow the existence of antiphase domains without local symmetry centers, but which are images of each other.

The interesting point of this structure is the existence of an ordered solution for all atoms with a scheme of hydrogen bonding which prevents at room temperature the existence of a plastic phase. Such a phase may however exist at higher temperatures and explains the phase changes observed before the decomposition point. To obtain more information on the motions of the ions in the different phases, additional experimental data, such as second moment and relaxation time NMR measurements, are required.

As far as the exact geometry of the OD_3^+ cation is concerned, it must be pointed out that the precision of the results obtained from the powder diffraction data is not very high and that the final values depend on the starting points used for the different refinements. Thus the O-D distance was found to vary from 0.91 to 1.05Å with the ODO angle varying from 116° to 92°. The correct values certainly lie between these extreme values. This is also reflected by the higher thermal parameters found for the deuterium and oxygen positions (see above) indicating high thermal motion of the OD_3^+ cation itself. For the O-H bond length in OH_3^+, a lower limit of 0.97Å appears more realistic for the following reasons. The bond length in free OH_2 is already 0.96Å and both the hydrogen-fluorine bridging and the increased $\overset{\delta-}{O}\text{-}\overset{\delta+}{H}$ polarity of the O-H bond in OH_3SbF_6 are expected to increase the O-H bond length. This bond weakening in OH_3^+ when compared to free OH_2 is also supported by the force constant calculations given below. The most likely range of the O-H bond length in these OH_3MF_6 salts is therefore 0.98-1.05Å which is in excellent agreement with the values of 1.013(8), 1.020(3), and 0.994(5)Å previously found for $OH_3^+CH_3C_6H_4SO_3^-$,[21] $OD_3^+CH_3C_6H_4SO_3^-$,[28] and $OH_3^+CF_3SO_3^-$,[29] respectively, by neutron diffraction, and values of 1.01 to 1.04Å for $OH_3^+NO_3^-$ and $OH_3^+ClO_4^-$, derived from wide line NMR measurements.[30]

The value of 1.19Å, previously reported[9] for the O-H bond length in $OH_3^+BF_4^-$, is based on X-ray data and therefore is deemed unreliable. It should be pointed out that the OH...F distances in $OH_3^+BF_4^-$ and $OD_3^+AsF_6^-$ are practically

identical (2.60Å). This suggests that r_{O-H} and r_{O-D} in these two compounds should also be similar.

The neutron model was tested against the X-ray data for OH_3SbF_6 but there was no improvement in the refinement or the appearance of the Fourier difference map.

Vibrational Spectra. Although many papers have been published on the vibrational spectra and force field of the oxonium ion,[4-9,31-45] many discrepancies exist among these data. Frequently, the infrared bands observed for the stretching modes are very broad, overlap and are complicated by Fermi resonance with combination bands. Also, the smooth transition from highly ionic OH_3^+ salts to proton transfer complexes and the interpretation of some of the more weakly ionized proton transfer complexes in terms of discrete OH_3^+ salts may have significantly contributed to the general confusion. As a consequence there is still considerable ambiguity[4] whether the antisymmetric or the symmetric OH_3^+ stretching mode has the higher frequency. Furthermore, the symmetric OH_3^+ deformation mode is generally very difficult to locate due to the great line width of the band.[46] Although vibrational spectra have previously been reported for OD_3^+,[32,34,38] they have been of little help to strengthen the vibrational assignments for the oxonium cation. Consequently, it was interesting to record the vibrational spectra of deuterated and partially deuterated OH_3^+ in salts containing well defined discrete oxonium cations. We hoped to verify the above described phase changes and to compare the experimentally observed spectra with the results from recent theoretical calculations [47-49] and with those of the isoelectronic ammonia analogues.[50-54]

The observed infrared and Raman spectra and the more important frequencies are given in Figures 3-7 and Table VI.

Room Temperature Spectra of OD_3AsF_6. Figure 3 shows the room temperature spectra of solid OD_3AsF_6. As can be seen, the bands are broad and show no splittings or asymmetry as expected for ions undergoing rapid motion in a plastic phase.[4,17,19] Based on their relative infrared and Raman intensities, the band at about 2450 cm^{-1} can be assigned with confidence to the

antisymmetric OD_3^+ stretching mode $\nu_3(E)$ and the band at about 2300 cm^{-1} to the symmetric OD_3^+ stretching mode $\nu_1(A_1)$. This assignment of $\nu_3 > \nu_1$ is further supported by all the other spectra recorded in this study (see below). Also, their frequency separation of about 150 cm^{-1} is very similar to that of 144 cm^{-1} found for isoelectronic ND_3.[50] Furthermore, a recent ab initio calculation for OD_3^+ also arrived (after applying the suggested -12.3% correction to all frequencies) at ν_3 being 165 cm^{-1} higher than ν_1 (see Table VII).[49] This finding that in a strongly hydrogen bridged oxonium salt ν_3 is higher than ν_1 disagrees with the previous suggestion that the order of the OH_3^+ stretching frequencies should invert when r_{X-Y} in X-H...Y becomes shorter than the van der Waals radius sum.[38]

The assignment of the 1192 cm^{-1} infrared and the 1178 cm^{-1} Raman band to the antisymmetric OD_3^+ deformation $\nu_4(E)$ is straight forward and again is in excellent agreement with the frequency values of 1191 and 1161 cm^{-1}, found for isoelectronic ND_3[50] and calculated for OD_3^+ by ab initio methods,[49] respectively (see Table VII).

The assignment of the last yet unassigned fundamental of OD_3^+, the symmetric deformation mode $\nu_2(A_1)$ is more difficult. Based on analogy with ND_3, this mode should occur at about 750 cm^{-1} and indeed the Raman spectrum of OD_3AsF_6 exhibits a band at 770 cm^{-1} of about the right intensity. The failure to observe a well defined infrared counterpart could possibly be due to its great linewidth. The ab initio calculations for $\nu_2(A_1)$ of OD_3^+ predict an intense infrared band at 549 cm^{-1}. Indeed the infrared spectrum of OD_3AsF_6 (trace A, Figure 3) shows a medium strong band at 580 cm^{-1}. However, we prefer to assign this band to $\nu_2(E_g)$ of AsF_6^- for the following reasons. This mode frequently becomes infrared active in many AsF_6^- salts. Furthermore, it has also been observed in OH_3AsF_6;[4] if it were due to OD_3^+, it would have been shifted in OH_3AsF_6 to a significantly higher frequency. This

assignment to ν_2 of AsF_6^- is also supported by the low-temperature infrared spectra of OH_3AsF_6 [4] and OD_3AsF_6 (Figure 4) both of which show two sharp bands of almost identical intensities and frequencies at about 580 and 560 cm^{-1}.

The remaining bands due to AsF_6^- in OD_3AsF_6 are in excellent agreement with those previously observed for OH_3AsF_6 and can be assigned accordingly.[4] IR: $\nu_3(F_{1u})$, 700; $\nu_4(F_{1u})$, 389 cm^{-1}. RA: $\nu_1(A_{1g})$, 682; $\nu_2(E_g)$, 560; $\nu_5(F_{2g})$, 363 cm^{-1}. Several weak bands in the spectrum of OD_3AsF_6 are marked by an asterisk. These are due to a small amount of OD_2H^+ and will be discussed below.

Low-Temperature Spectra of OD_3AsF_6. Figure 4 shows the low-temperature spectra of OD_3AsF_6. The most prominent changes from the room temperature spectra are the pronounced sharpening of all bands accompanied by splittings. As discussed above, these changes are caused by freezing of the ion motions. The change from a plastic phase to an ordered one, occurring based on the DSC measurements in the -7 to +2°C temperature range was confirmed by Raman spectroscopy. As can be seen from Figure 5, the freezing out of the ion motion occurs indeed within the very narrow temperature range.

Compared to the room temperature spectra, the low-temperature spectra do not provide much additional information on the fundamental vibrations of OD_3^+. The $\nu_1(A_1)$ fundamental is shown to occur at a lower frequency than $\nu_3(E)$, and $\nu_4(E)$ shows a splitting into two components in the infrared spectrum. The $\nu_2(A_1)$ deformation mode is again difficult to locate but clearly cannot be attributed to the 582 cm^{-1} infrared band for the above given reasons.

From the AsF_6^- part of the spectra some conclusions concerning the possible site symmetry of AsF_6^- might be reached. All degeneracies appear to be lifted for the fundamentals and the bands are not mutually exclusive. This eliminates all centrosymmetric space groups and site symmetries, such as O_h, T_h or C_{3i}. The highest possible site symmetry appears to be C_3, in agreement with our triply hydrogen bonded model possessing AsF_6^- ions with three shorter and three longer As-F bonds. Since that unit cell contains more than one molecule, additional splittings are possible due to in-phase out-of-phase coupling effects within the unit cell.

The low-temperature spectra of OD_3AsF_6 show a medium strong IR band at 341 cm^{-1} and a Raman band at 329 cm^{-1}. These bands cannot be assigned to AsF_6^- because their frequencies are too low for ν_4 and also they were not observed in the low-temperature spectra of OH_3AsF_6.[4] In OH_3AsF_6, however, two corresponding bands were observed at 467 cm^{-1}(IR) and 480 cm^{-1}(RA).[4] Since their average frequency values, 335 and 474 cm^{-1}, respectively, are exactly in a ratio of $1:\sqrt{2}$, these bands must involve the hydrogen atoms and therefore are assigned to the D...F and H...F stretching modes, respectively. As expected, these bands due to H...F stretching are not observed in the plastic phase, room temperature spectra due to rapid motion of the ions.

Using a simple diatomic model and the average observed frequency values ($\nu_{H...F}$ = 474 and $\nu_{D...F}$ = 335 cm^{-1}), the corresponding force constants are f_{HF} = 0.1258 mdyn/Å and f_{DF} = 0.1204 mdyn/Å, respectively. Their averaged value (0.1231 mdyn/Å) corresponds to a hydrogen bridge bond energy of 1.77 kcal mol^{-1}, indicative of a weak hydrogen bond.

Spectra of OD_3SbF_6, OH_3SbF_6 and Partially Deuterated OH_3SbF_6. Figure 6 shows the room temperature vibrational spectra of OD_3SbF_6, OH_3SbF_6 and partially deuterated OH_3SbF_6. Although the Raman lines due to SbF_6^- (670, 590, 555 and 282 cm^{-1} in trace E) are broadened, the 670 cm^{-1} line has a pronounced shoulder at 644 cm^{-1}, the $\nu_2(E_g)$ mode is split into its two degenerate components (see Figure 5), and the D...F stretching mode at 355 cm^{-1} (trace E of Figure 6) and H...F stretching mode at 487 cm^{-1} (trace A of Figure 6) are observed. All these features clearly indicate that OD_3SbF_6 and OH_3SbF_6 are ordered at room temperature, thus confirming the above given DSC and neutron diffraction data.

The assignments for OD_3^+ in its SbF_6^- salt can be made by complete analogy to those given above for OD_3AsF_6. The increased splitting of the 2430 and 2330 cm^{-1} bands and their relative infrared intensities[49] (trace D of Figure 6) lend further support to the $\nu_3 > \nu_1$ assignment for the oxonium salts. On cooling (see Figure 7) all the important spectral features are retained,

but become more evident due to better resolution caused by the narrower linewidths. Thus the D...F stretching vibrations at 380 cm^{-1} become very prominent in the infrared spectra.

An analysis of the bands attributable to SbF_6^- (IR: 668, 645, 590, 554, 548, 285sh, 270sh, 261; RA: 680sh, 673, 650sh, 640, 586, 554, 291sh, 287sh, 281, 265sh) shows again that the site symmetry can be at best C_3. Thus the vibrational spectra appear to be compatible with a space group, such as $I2_13$ which was chosen for the above given neutron diffraction structure analysis.

Assignments for OD_2H^+ and ODH_2^+. The vibrational spectra of the OD_3^+ salts showed bands at about 3160, 2920 and 1470 cm^{-1}, marked by an asterisk in Figure 3, which could not readily be attributed to combination bands of OD_3^+. Assignment of the 1470 cm^{-1} infrared band to the antisymmetric stretching mode of HF_2^- is also unsatisfactory, because the band was also observed in the Raman spectrum which in turn did not show the expected symmetric HF_2^- stretching mode at 600 cm^{-1}. Furthermore, $OD_3^+SbF_6^-$ should result in the formation of DF_2^- and not of HF_2^-. Consequently, we have examined the possibility of these bands being due to small amounts of incompletely deuterated oxonium ions by recording the spectra of partially deuterated OH_3SbF_6. As can be seen from trace B of Figure 6, the intensity of the band at about 3160, 2920 and 1470 cm^{-1} has increased strongly for the partially deuterated sample and therefore these bands are assigned to the OD_2H^+ cation. The observed frequencies closely correspond to those of isoelectronic ND_2H [51-54] and the ab-initio calculated OD_2H^+ values[49] (see Table VIII). Consequently the 3160 and 1470 cm^{-1} bands are assigned to the OH stretching mode and the antisymmetric (A') OD_2H deformation mode, respectively of OD_2H^+. The 2920 cm^{-1} band can readily be assigned to the first overtone of the 1470 cm^{-1} band being in Fermi resonance with the OH stretching mode. The antisymmetric and symmetric OD_2 stretching modes of

OD_2H^+ are expected to have frequencies of about 2400 and 2300 cm^{-1},[49,51-54] respectively, and therefore are hidden underneath the intense OD_3^+ stretching modes. The antisymmetric (A")OD_2H^+ deformation mode is expected[49,51-54] to have a frequency between 1190 and 1250 cm^{-1} and therefore can be assigned to the infrared band at 1220 cm^{-1} observed in Trace B of Figure 6.

In addition to the bands attributed to OD_3^+ and OD_2H^+, the infrared spectrum of the partially deuterated OH_3SbF_6 sample (calcd. product distribution: OD_3^+51.68, OD_2H^+38.16, ODH_2^+9.33, and OH_3^+0.77mol%) exhibits two bands at 1601 and 1388 cm^{-1} (see trace B of Figure 6). These band are in excellent agreement with our expectations[49,51-54] (see Table VIII) for δas(A") and δas(A'), respectively, of ODH_2^+ and are assigned accordingly. The OD and OH_2 stretching modes of ODH_2^+ are again buried in the broad intense bands centered at about 2400 and 3300 cm^{-1} and therefore cannot be located with any reliability. The symmetric deformation modes of OD_2H^+ and ODH_2^+ are probably giving rise to the strong shoulder in the 800-900 cm^{-1} range (trace B of Figure 6), but cannot be located precisely due to their broadness.

The above assignments for OD_2H^+ and ODH_2^+ are further substantiated by the low-temperature spectra shown in Figures 4 and 7, with the decreased line widths allowing a more precise location of the individual frequencies. Most of the infrared bands observed in the 320-510 cm^{-1} region for the low-temperature spectra of the different oxonium SbF_6^- salts are attributed to the D...F and H...F stretching modes of the hydrogen bridges.

In summary, most of the features observed for the vibrational spectra of the oxonium salts can satisfactorily be accounted for by the assumption of disordered higher-temperature and ordered, hydrogen bridged, lower-temperature phases. Reasonable assignments can be made for the series OH_3^+, ODH_2^+, OD_2H^+, OD_3^+ (see Table VI) which are in excellent agreement with

those of the corresponding isoelectronic ammonia molecules[51-54] and the results of recent ab-initio calculations[49] (see Tables VII and VIII). The only discrepancy between the ab-initio calculations and the experimental data exists in the area of the symmetric deformation modes. This could be caused by the low barrier to inversion in OH_3^+ [49].

Force Constants. In view of our improved assignments for the oxonium cation, it was interesting to redetermine its force field. The frequencies and assignments given in Table VIII, a bond length of 1.01Å and a bond angle of 110° were used to calculate a valence force field of OD_3^+ using a previously described method[4] to obtain an exact fit between calculated and observed frequencies. The results of these computations are summarized in Table IX.

Since isotopic shifts obtained by light atom substitution, such as H-D, are virtually useless for the determination of a general valence force field,[55] approximating methods were used. Three different force fields were computed for OD_3^+ to demonstrate that for a vibrationally weakly coupled system, such as OD_3^+, the choice of the force field has little influence on its values. Our preferred force field is that assuming F_{22} and F_{44} being a minimum. This type of force field has previously been shown[56] to be a good approximation to a general valence force field for vibrationally weakly coupled systems. As can be seen from Table IX, the force field obtained in this manner is indeed very similar to the general force field previously reported[57] for ND_3 and NH_3. The fact that the force constants of OD_3^+ deviate somewhat from those of OH_3^+ is mainly due to the broadness of the OH_3^+ vibrational bands and the associated uncertainties in their frequencies. Since the stretching frequencies of OD_3^+ are more precisely known than those of OH_3^+, the OD_3^+ force field should be the more reliable one. The fact that F_{12} in NH_3 and ND_3 is somewhat larger than the value obtained for F_{12} in our F_{22}=Min force field is insignificant because in the published[57] NH_3 force field F_{12} was not well determined and was con-

sequently assumed to equal $-2F_{34}$. The fact that the stretching force constant f_r in OD_3^+ is slightly lower and the deformation constant f_α in OD_3^+ is slightly higher than those in ND_3 is not unexpected. The ND_3 frequencies were those of the free molecule, whereas the OD_3^+ values are taken from the ionic solid $OD_3^+AsF_6^-$. In this solid, D-F bridging occurs (see above), hereby lowering the OD stretching and increasing the deformation frequencies. As secondary effects, the higher electronegativity of oxygen and the positive charge in OD_3^+ are expected to increase the polarity of the O-D bonds, thereby somewhat decreasing all the frequencies. These explanations can well account for the observed differences.

For the bending force constant f_α values of 0.563 and 0.542 mdyn $\text{Å}/\text{radian}^2$ were obtained for OD_3^+ and OH_3^+, respectively. These values are in excellent agreement with the value of 0.55 mdyn $\text{Å}/\text{radian}^2$ obtained for OH_3^+ by an ab-initio calculation.[47]

In summary, the results from our normal coordinate analysis lend strong support to our analysis of the vibrational spectra. They clearly demonstrate the existence of discrete OH_3^+ ions which in character closely resemble the free NH_3 molecule, except for some secondary effects caused by hydrogen-fluorine bridging.

Conclusion. The results of this study show that OD_3AsF_6 exists at room temperature in a plastic phase, whereas OD_3SbF_6 has an ordered structure. Based on diffraction data and vibrational spectra, a structural model is proposed for the ordered phase of OD_3SbF_6. More experimental data are needed to define the exact nature of the ion motions and the associated phase changes in these salts. Many of the observations made in this study are in poor agreement with previous reports for other oxonium salts and cast some doubt on the general validity of some of the previous conclusions.

Due to their good thermal stability, oxonium salts of complex fluoro cations are well suited for further experimental studies.

Acknowledgement. The authors are indebted to Drs. C. Schack, R. Wilson, and W. Wilson of Rocketdyne, Dr. P. Meriel of CEN Saclay, and Dr. P. Aldebert of ILL Grenoble for their help with experiments. One of us (KOC) thanks the U.S. Army Research Office and the Office of Naval Research for financial support.

References

(1) Rocketdyne

(2) CEN Saclay

(3) University of Leicester

(4) Christe, K. O.; Schack, C. J.; Wilson, R. D. Inorg. Chem. 1975, 14,2224.

(5) Masson, J. P.; Desmoulin, J. P.: Charpin, P.; Bougon, R. Inorg. Chem. 1976, 15,2529.

(6) Christe, K. O.; Wilson, W. W.; Schack, C. J. J. Fluor. Chem. 1978, 11,71.

(7) Selig, H.; Sunder, W. A.; Disalvo, F. A.; Falconer, W. E. J. Fluor. Chem. 1978, 11,39.

(8) Selig. H.; Sunder, W. A.; Schilling, F. C.; Falconer, W. E. J. Fluor. Chem. 1978, 11,629.

(9) Cohen, S.; Selig, H.; Gut, R. J. Fluor. Chem. 1982, 20,349.

(10) Mootz, D.; Steffen, M. Z. anorg. allgem. Chem. 1981, 482,193.

(11) Christe, K. O.; Wilson, R. D.; Schack, C. J. Inorg. Synth., in press.

(12) Shamir, J.; Binenboym, J. Inorg. Chim. Acta 1968, 2,37.

(13) Plyler, E. K.; Danti, A.; Blaine, L. R.; Tidwell, E. D. J. Res. Natl. Bur. Stand., Sect. A 1960, 64A,841.

(14) International Union of Pure and Applied Chemistry. "Tables of Wavenumbers for the Calibration of Infrared Spectrometers"; Butterworths: Washington, DC, 1961.

(15) Claassen, H. H.; Selig, H.; Shamir, J. Appl. Spectrosc. 1969, 23,8.

(16) Miller, F. A.; Harney, B. M. J. Appl. Spectrosc. 1970, 24,271.

(17) Griffiths, J. E.; Sunder, W. A. J. Chem. Phys. 1982, 77,1087.

(18) Young, A. R.; Hirata, T.; Morrow, S. I. J. Am. Chem. Soc. 1964, 86,20.

(19) Naulin, C.; Bougon, R. J. Chem. Phys. 1976, 64,4155.

(20) Gafner, G.; Kruger, G. J. Acta Cryst. 1974, B30,250.

(21) Lundgren, J. O.; Williams, J. M. J. Chem. Phys. 1973, 58,788.

(22) APL program written by G. Langlet.

(23) Ibers, J. A.; Hamilton, W. C. J. Chem. Phys. 1966, 44, 1748.

(24) McKee, D. E.; Bartlett, N. Inorg. Chem. 1973, 12,2738.

(25) Sheldrick, G. M.; "Shelx a Program for Structure Determination," Univ. of Cambridge, England, 1976.

(26) Rietveld, H. M. J. Appl. Cryst. 1969, 2,65.

(27) Heyns, A. M.; Pistorius, C. W. F. T. Spectrochim. Acta, Part A 1976, 32A,535.

(28) Finholt, J. E.; Williams, J. M. J. Chem. Phys. 1973, 59,5114.

(29) Lundgren, J. O.; Tellgren, R.; Olovsson, I. Acta Cryst. B 1978, B34,2945.

(30) Herzog-Cance, M. H.; Potier, J.; Potier, A. Adv. Mol. Relax. Interact. Proc. 1979, 14,245.

(31) Bethell, D. E.; Sheppard, N. J. Chem. Phys. 1953, 21,1421.

(32) Ferriso, C. C.; Hornig, D. F. J. Am. Chem. 1953, 75,4113 and J. Chem. Phys. 1955, 23,1464.

(33) Fournier, M.; Roziere, J. C. R. Hebd. Seances Acad. Sci., Ser. C, 1970, 270,729.

(34) Fournier, M.; Mascherpa, G.; Rousselet, D.; Potier, J. C. R. Hebd. Seances Acad. Sci., Ser. C, 1969, 269,279.

(35) Millen, D. J.; Vaal, E. G. J. Chem. Soc. 1956, 2913.

(36) Taylor, R. C.; Videale, G. L. J. Amer. Chem. Soc. 1956, 78,5999.

(37) Mullhaupt, J. T.; Hornig, D. F. J. Chem. Phys. 1956, 24,169.

(38) Basile, L. J.; La Bonville, P.; Ferraro, J. R.; Williams, J. M. J. Chem. Phys. 1974, 60,1981.

(39) Ferraro, J. R.; Williams, J. M.: La Bonville, P. Appl. Spectrosc. 1974, 28,379.

(40) Huong, P. V.; Desbat, B. J. Raman Spectrosc. 1974, 2,373.

(41) Gilbert, A. S.; Sheppard, N. J. Chem. Soc. Faraday Trans. II 1973, 69,1628.

(42) Savoie, R.; Giguere, P. A. J. Chem. Phys. 1964, 41,2698.

(43) Schneider, M.; Giguere, P. A. C. R. Hebd. Seances Acad. Sci., Ser. C, 1968, 267,551.

(44) Desbat, B.; Huong, P. V. Spectrochim. Acta, Part A 1975, 31A,1109.

(45) Giguere, P. A.; Turrell, S. J. Amer. Chem. Soc. 1980, 102,5473 and Canad. J. Chem. 1976, 54,3477.

(46) Giguere, P. A.; Guillot, J. G. J. Phys. Chem. 1982, 86,3231.

(47) Allavena, M.; Le Clec'h, E. J. Mol. Structure 1974, 22,265.

(48) Bunker, P. R.; Kraemer, W. P.; Spirko, V. J. Mol. Spectrosc. 1983, 101,180.

(49) Colvin, M. E.; Raine, G. P.; Schaefer, H. F.; Dupuis, M. J. Chem. Phys. 1983, 79,1551.

(50) Shimanouchi, T., "Tables of Molecular Vibrational Frequencies," Nat. Stand. Ref. Data Ser., Nat. Bur. Stand. (U.S.) 1972, 39,15.

(51) Whitmer, J. C. J. Chem. Phys. 1972, 56,1050.

(52) Wolff, H.; Rollar, H. G.; Wolff, E. J. Chem. Phys. 1971, 55,1373.

(53) Reding, F. P.; Hornig, D. F. J. Chem. Phys. 1951, 19,594 and 1955, 23,1053.

(54) Thornton, C.; Khatkale, M. S.; Devlin, J. P. J. Chem. Phys. 1981, 75,5609.

(55) Mohan, N.; Mueller, A.; Nakamoto, K. Advances in Infrared and Raman Spectrosc. 1975, 1,180.

(56) Sawodny, W. J. Mol. Spectrosc. 1969, 30,56.

(57) Shimanouchi, T.; Nakagawa, I.; Hiraishi, J.; Ishii, M. J. Mol. Spectrosc. 1966, 19,78.

Table I. X-ray Diffraction Powder Pattern of OH_3AsF_6 at -153°C[a]

d obs (Å)	int	d obs (Å)	int
6.35	vw	2.024	ms
4.95	s	2.010	m
4.72	s	1.942	m
4.12	w	1.913	vvw
3.87	w	1.877	ms
3.749	ms	1.871	w
3.730		1.802	vw
3.473	m	1.775	vw
3.225	m	1.769	vw
3.163	m	1.739	vw
3.029	mw	1.712	w
2.845	m	1.695	w
2.837		1.659	vw
2.596	w	1.648	mw
2.530	vw	1.612	w
2.362	vvw	1.585	mw
2.139	w	1.581	vw
2.061	m		
2.055			

[a]CuKα radiation and Ni filter

Table II. Neutron Diffraction Powder Patterns of the Face Centered Cubic, Room Temperature Phases of OH_3AsF_6, OD_3AsF_6 and O_2AsF_6 [a]

h k l	OH_3AsF_6		OD_3AsF_6	O_2AsF_6
	int calc	int obs	int obs	int obs
111	1100	1127	12	200
200	177	174	1033	1000
220	11	-	177	215
311	5	-	137	210
222	0	-	19	45
400	2	-	12	20
331	5	-	-	-
420	66	71	38	90
422	100	92	26	100
511/333	5	-	16	35

[a] Intensities in arbitrary units

Table III. Room-Temperature X-ray Powder Data for $^{-}OH_3SbF_6$

d_{obsd}, Å	d_{calcd}, Å	Intens	h	k	l
5.04	5.04	vs	2	0	0
3.56	3.57	vs	2	2	0
2.909	2.912	mw	2	2	2
2.691	2.696	w	3	2	1
2.519	2.522	mw	4	0	0
2.374	2.378	w	4	1	1
2.254	2.256	m	4	2	0
2.149	2.151	mw	3	3	2
2.060	2.059	s	4	2	2
1.979	1.978	w	4	3	1
1.784	1.783	ms	4	4	0
1.682	1.681	ms	6	0	0, 4 4 2
1.637	1.636	vw	5	3	2
1.596	1.595	ms	6	2	0
1.519	1.521	ms	6	2	2
1.456	1.456	w	4	4	4
1.398	1.399	ms	6	4	0
1.372	1.373	vw	6	3	3
1.349	1.348	ms	6	4	2
1.282	1.281	vw	7	3	2, 6 5 1
1.262	1.261	vw	8	0	0
1.225	1.223	m	8	2	0, 6 4 4
1.189	1.189	m	8	2	2, 6 6 0
1.159	1.157	w	6	6	2
1.129	1.128	m	8	4	0
1.103	1.101	m	8	4	2

cubic, a = 10.09A, V = 1027.2Å^3, Z = 8, ρcalcd = 3.296 gcm^{-3}, CuK_α radiation, Ni filter

Table V. X-ray and Neutron Powder Patterns of OD_3SbF_6 at Room Temperature

h k l	X-ray	Neutron	h k l	X-ray	Neutron
200	100	6	710/550/543	-	1
211	-	2	640	11	8
220	70	100	721/633/552	1	8
222	13	8	642	21	9
321	3	30	730	-	3
400	7	2	732/651	2	18
411/330	6	13	800	4	-
420	17	17	811/741/554	-	7
332	4	22	820/644	11	9
422	36	18	653	-	3
431/510	3	13	822/660	10	2
440	19	14	831/750/743	-	4
433/530	21	3	662	4	-
442/600	2	7	752	-	3
611/532	2	9	840	6	2
620	21	3			
541	1	14			
622	12	5			
631	-	2			
444	4	4			

Table VI. Vibrational Spectra

obsd freq, cm^{-1}, and rel intens[a]				assignments (point group)[b]			
OD_3AsF_6[c]							
25°		-196°	-100°				
IR	RA	IR	RA	$OD_3^+(C_{3v})$	$OD_2H^+(C_s)$	$AsF_6^-(O_h)$	
3170mw,br		3170 m 3120 m			νOH(A')		
2910,vw,br		2920 w 2903 w			2δas(A')		
2450vs,br	2400sh	2485s	2490sh	νas(E)	νasOD$_2$(A")		
		2410vs	2400sh	2δas(A$_1$)	νsOD$_2$(A')		
2290s,br	2300(0.3)	2320s	2305(0.6)	νs(A$_1$)			
1471mw	1440(0+)	1462 m 1448 m			δas(A')		
		1222vw			δas(A")		
1192ms	1178(0.3)	1197 ms 1190 ms	1182(0.3)	δas(E)			
		1030m					
		882vw					
	810sh	808m					
	770(0.2)	750sh		δs(A$_1$)			
			712sh				
700vs,br		680vs(br)	704(10)			νas(F$_{1u}$)	
	682(10)		667(7.9)			νs(A$_{1g}$)	
580m,br		582s					
	560(1.6)	556s	555(3.3)			νs(Eg)	
		510w			νF...H		
		410sh			νF...D		
389s		387vs				δas(F$_{1u}$)	
		372sh	377(1.2)				
	363(3.6)		367(1.9)			δs(F$_{2g}$)	
		358mw	359(2.9)				
		341s		νF...D			
		325sh	329(0.8)				

(a) Uncorrected Raman intensities. (b) Idealized point groups were assumed for the reasonable for the disordered phases but is not valid for the ordered phases in the ions is C_3 or lower. (c) The spectra of these compounds contain bands due small amount of H_2O in the D_2O starting material (~0.4%) and from handling of

rational Spectra of OD_3AsF_6, OD_3SbF_6 and Their Partially Deuterated Analogues

obsd freq, cm^{-1}, and rel inten[a]						assignments (point group)[b]		
OD_3SbF_6[c]				$OD_nH_{3-n}SbF_6$				
25°		-196°	-110°	25°	-196°	$OD_3^+(C_{3v})$	$OD_2H^+(C_s)$	$ODH_2^+(C_s)$
IR	RA	IR	RA	IR				
3165mw,br		3160m 3120m		3400-3000vs,br	3150m		νOH(A')	νasOH₂(A') νsOH₂(A')
2925		2935mw		2930m	2980w 2935mw		2δas(A')	
2430vs,br		2575sh 2500m 2415s	2500sh 2400sh	2440vs,br	2510m 2410s	νas(E)	νasOD₂(A")	
2330s,br	2295(0.2)	2340s 2295w	2335(0+) 2295(0.6)	2320vs,br	2340m 2295w	2δas(A₁) νs(A₁)	νsOD₂(A')	νOD(A')
1601m		1523mw		1601m	1613mw 1525w			δas(A")
1475mw	1480mw		1475ms	1481ms			δas(A')	
		1228w	1388w	1398w				δas(A')
1195mw	1199(0+)	1199s		1220w 1195ms	1229mw 1199ms	δas(E)	δas(A")	
	742(0+)		680sh	900-800sh,br	870sh 750sh	δs(A₁)	δs(A')	
670vs,br	670(10)	668vs	673(10) 650sh	680vs,br	670vs			
	644sh	645s	640(4.1)		643vs			
565m,br	590(0.8)	590mw 554m	586(0.7)	565m,br	590mw 564m			
	555(1.5)	548ms	554(1.8)		558ms			
		510vw 441m 410sh			510m 441ms 411m		νF...H νF...D	
	355(0.2)	380s 370sh	375(0.3)		381s			
		333m 317m			353w 334w 319m	νF...D		
	282(4.5)	290sh 275sh 261vs	291sh 287sh 281(4.4) 265sh		290sh 274sh 262vs			

re assumed for the ions; this approximation is
ordered phases in which the site symmetry of
contain bands due to some OD_2H^+ resulting from a
from handling of the IR samples.

Their Partially Deuterated Analogues

$OD_nH_{3-n}SbF_6$			assignments (point group)[b]			
-110°	25°	-196°	$OD_3^+(C_{3v})$	$OD_2H^+(C_s)$	$ODH_2^+(C_s)$	$SbF_6^-(O_h)$
RA	IR					
	3400-3000vs,br	3150m		νOH(A')	νasOH$_2$(A") / νsOH$_2$(A')	
	2930m	2980w 2935mw		2δas(A')		
2500sh 2400sh	2440vs,br	2510m 2410s	νas(E)	νasOD$_2$(A")		
2335(0.4) 2295(0.6)	2320vs,br	2340m 2295w	2δas(A$_1$) νs(A$_1$)	νsOD$_2$(A')	νOD(A')	
	1601m	1613mw 1525w			δas(A")	
1475ms	1481ms			δas(A')		
1388w	1398w				δas(A')	
	1220w	1229mw		δas(A")		
	1195ms 900-800sh,br	1199ms 870sh 750sh	δas(E) δs(A$_1$)	δs(A')		
680sh						
673(10) 650sh	680vs,br	670vs				νas(F_{1u}),νs(A_{1g})
640(4.1)		643vs				
586(0.7) 554(1.8)	565m,br	590mw 564m 558ms				νs(E_g)
		510m 441ms 411m		νF...H νF...D		
375(0.3)		381s 353w 334w 319m	νF...D			
291sh 287sh		290sh				δas(F_{1u}) δs(F_{2g})
281(4.4) 265sh		274sh 262vs				

ion is
ry of
g from a

Table VII. Frequencies (cm^{-1}), Frequency Shifts on Deuteration, and Relative Infrared Intensities of OD_3^+ and OH_3^+ Compared to Those of Gaseous ND_3 and NH_3[a] and to the Results from Ab-Initio Calculations[b]

Assignment for point group C_{3v}		Approximate description of mode	OD_3^+ obsd	OH_3^+ obsd	$\nu OH_3^+ : \nu OD_3^+$	ND_3	NH_3	$\nu NH_3 : \nu ND_3$	OD_3^+ calcd	OH_3^+ calcd	$\nu OH_3^+ C : \nu OD_3^+ C$
A_1	ν_1	νsym XY_3	2300(m)	3150(m)	1.37	2420	3336	1.38	2424 (0.6)	3411(1.0)	1.41
	ν_2	δsym XY_3	715	900(m,br)	1.26	748	950	1.27	549(6.6)	725(13.9)	1.32
E	ν_3	νasym XY_3	2450(vs)	3300(vs)	1.35	2564	3444	1.34	2589(7.0)	3516(13.5)	1.36
	ν_4	δasym XY_3	1182(ms)	1620(ms)	1.37	1191	1626	1.37	1161(1.3)	1598(3.2)	1.38

[a]Data from Ref. 50.

[b]Data from Ref. 49 after application of the suggested -12.3% frequency correction.

Table VIII. Frequencies (cm^{-1}) and Relative Infrared Intensities of OD_2H^+ and ODH_2^+ Compared to Those of Solid ND_2H and NHD_2[a] and to the Results of Ab-Initio Calculations[b]

Assignment for point group C_s		Approximate description of mode for XY_2Z	OD_2H^+ clcd	OD_2H^{+c} obsd	ND_2H obsd	ODH_2^+ clcd	ODH_2^{+c} obsd	NDH_2 obsd
A'	ν_1	XZ stretch	3484(9.9)	3150(vs)	3329(s)	2532(4.4)		2447(s)
	ν_2	sym XY_2 stretch	2476(2.1)		2392(m)	3450(5.8)		3300(m)
	ν_3	asym deformation	1447(2.7)	1481(mw)	1476(mw)	1344(1.7)	1398(w)	1393(w)
	ν_4	sym deformation	611(9.0)		905(vs)	671(11.5)		992(vs)
A"	ν_5	asym XY_2 stretch	2589(7.2)		2501(vs)	3516(13.5)		3359(vs)
	ν_6	asym deformation	1186(1.2)	1229(w)	1254(w)	1580(3.4)	1613(mw)	1602(mw)

(a) Data from ref 52. (b) Data from ref 49 after application of the suggested -12.3% frequency correction. (c) Frequency values taken from the low-temperature IR spectra of the SbF_6^- salts.

Table IX. Symmetry and Internal Force Constants[a] of OD_3^+ Compared to Those of OH_3^+, NH_3 and ND_3[b]

		OD_3^+			OH_3^+	NH_3-ND_3
	Forcefield[c]	DFF	F_{22} and F_{44} ≡ Min	NH_3TR	F_{22} and F_{44} ≡ Min	GVFF
A_1	$F_{11}=f_r+2f_{rr}$	6.030	6.0440	6.085	5.7783	6.4540
	$F_{22}=f_\alpha+2f_{\alpha\alpha}$	0.4868	0.4866	0.4997	0.4382	0.4049
	$F_{12}=2f_{r\alpha}+f_{r\alpha'}$	0	0.0527	0.3244	0.0242	0.3244
E	$F_{33}=f_r-f_{rr}$	6.0595	6.1194	6.133	5.9696	6.4732
	$F_{44}=f_\alpha-f_{\alpha\alpha}$	0.6041	0.6010	0.6011	0.5934	0.6161
	$F_{34}=-f_{r\alpha}+f_{r\alpha'}$	0	-0.1228	-0.1622	-0.0654	-0.1622
	f_r	6.0497	6.0943	6.117	5.9058	6.4668
	f_{rr}	-0.0098	-0.0251	-0.016	-0.0638	-0.0064
	f_α	0.5650	0.5629	0.5673	0.5417	0.5457
	$f_{\alpha\alpha}$	-0.0391	-0.0381	-0.0338	-0.0517	-0.0704
	$f_{r\alpha}$	0	0.0582	0.1622	0.0355	0.1622
	$f_{r\alpha'}$	0	-0.0646	0	-0.0299	0

(a) Stretching constants in mdyn/Å, deformation constants in mdyn Å/radian^2, and stretch-bend interaction constants in mdyn/radian. The following bond angles and lengths were used, OD_3^+ and OH_3^+, 110° and 1.01Å, NH_3, 107° and 1.01Å, and the bending coordinates were weighted by unit (1Å) distance. Frequency values used: OD_3^+, ν_1=2300, ν_2=715, ν_3=2450, ν_4=1182; OH_3^+, ν_1=3150, ν_2=900, ν_3=3300, ν_4=1620 cm^{-1}. (b) Values from ref 57 assuming $F_{12}=-2F_{34}$. (c) The potential energy distribution for OD_3^+ showed all fundamentals to be close to or 100% characteristic with the largest amount of mixing being observed for ν_4 in the NH_3 transfer force field of OH_3^+.

Diagram Captions

Figure 1. - Neutron powder diffraction diagram of OD_3SbF_6 at ambient temperature, traces A and B, observed and calculated profiles, respectively.

Figure 2. - ORTEP stereoview of the structure of OD_3SbF_6. The bridging F_2 atoms are differentiated from the non-bridging F_1 atoms by smaller circles marked by traces.

Figure 3. - Vibrational spectra of solid OD_3AsF_6 at room temperature. Trace A, infrared spectrum of the solid pressed between AgCl disks. The broken line indicates absorption due to the window material. The bands marked by an asterisk are due to OD_2H^+ mainly formed during sample handling. Traces B and C, Raman spectra recorded at two different sensitivities with a spectral slit width of 3 and 8 cm^{-1}, respectively.

Figure 4. - Vibrational spectra of solid OD_3AsF_6 at low-temperature. Trace A, infrared spectrum of the solid pressed between AgCl disks and recorded at -196°C. Traces B and C, Raman spectra recorded at -100°C at two different sensitivities.

Figure 5. - Raman spectra of OD_3SbF_6 and OD_3AsF_6 at different temperature contrasting the slow gradual temperature induced line broadening for the ordered OD_3SbF_6 phase against the abrupt change within a narrow temperature range for OD_3AsF_6 caused by the transition from an ordered to a plastic phase.

Figure 6. - Vibrational spectra of solid OD_3SbF_6, OH_3SbF_6 and partially deuterated OH_3SbF_6 at room temperature. Trace A, IR spectrum of OH_3SbF_6; trace B, IR spectrum of partially deuterated OH_3SbF_6 containing about equimolar amounts of OD_3SbF_6, and OD_2HSbF_6 and smaller amounts of ODH_2SbF_6; trace C, IR spectrum of OD_3SbF_6 containing a significant amount of OD_2HSbF_6 formed during sample handling; trace D, IR spectrum of OD_3SbF_6 containing only a small amount of OD_2HSbF_6; traces E and F, RA spectra of OD_3SbF_6 recorded at two different sensitivities.

Figure 7. - Vibrational spectra of solid OD_3SbF_6 and partially deuterated OH_3SbF_6 at low temperature. Traces A and B, infrared spectra of partially deuterated OH_3SbF_6 and of OD_3SbF_6, respectively, between AgBr windows; traces C and C, Raman spectra recorded at two different sensitivities.

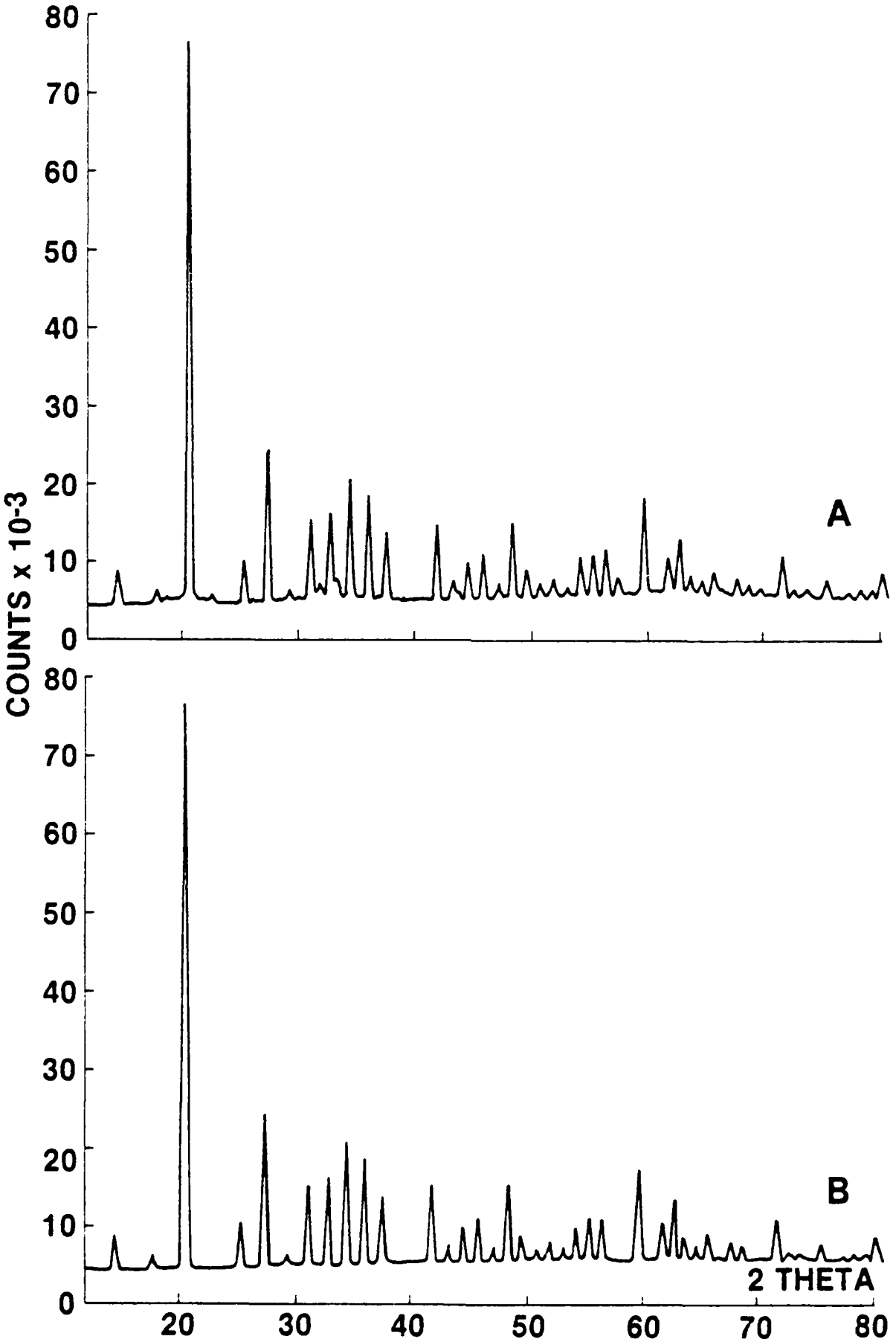

FIGURE 1.

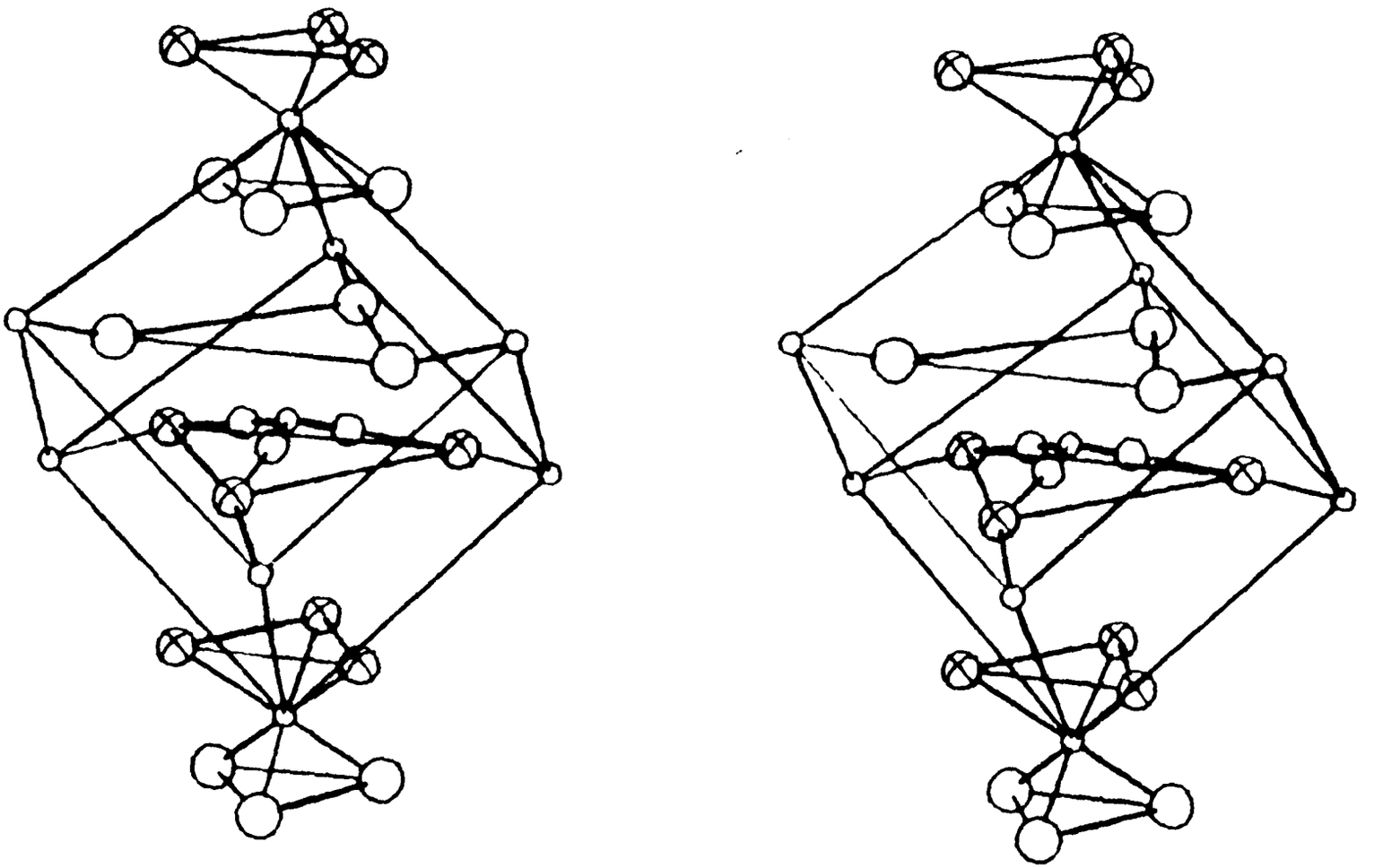

FIGURE 2.

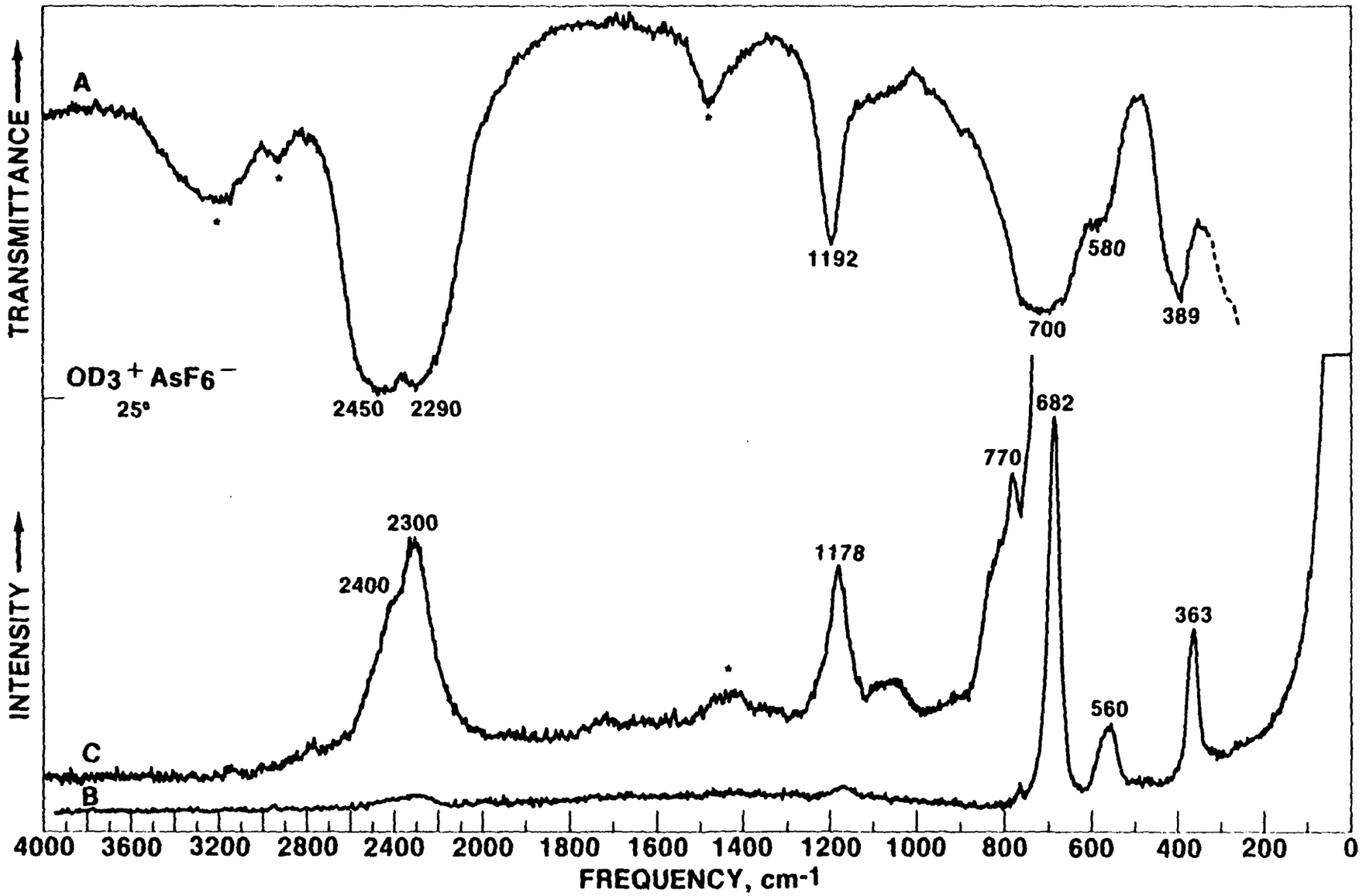
TRANSMITTANCE
A
1192
580
700
389
OD3 + AsF6 −
25°
2450
2290
INTENSITY
2300
2400
1178
770
682
363
560
C
B
4000 3600 3200 2800 2400 2000 1800 1600 1400 1200 1000 800 600 400 200 0
FREQUENCY, cm-1

FIGURE 3.

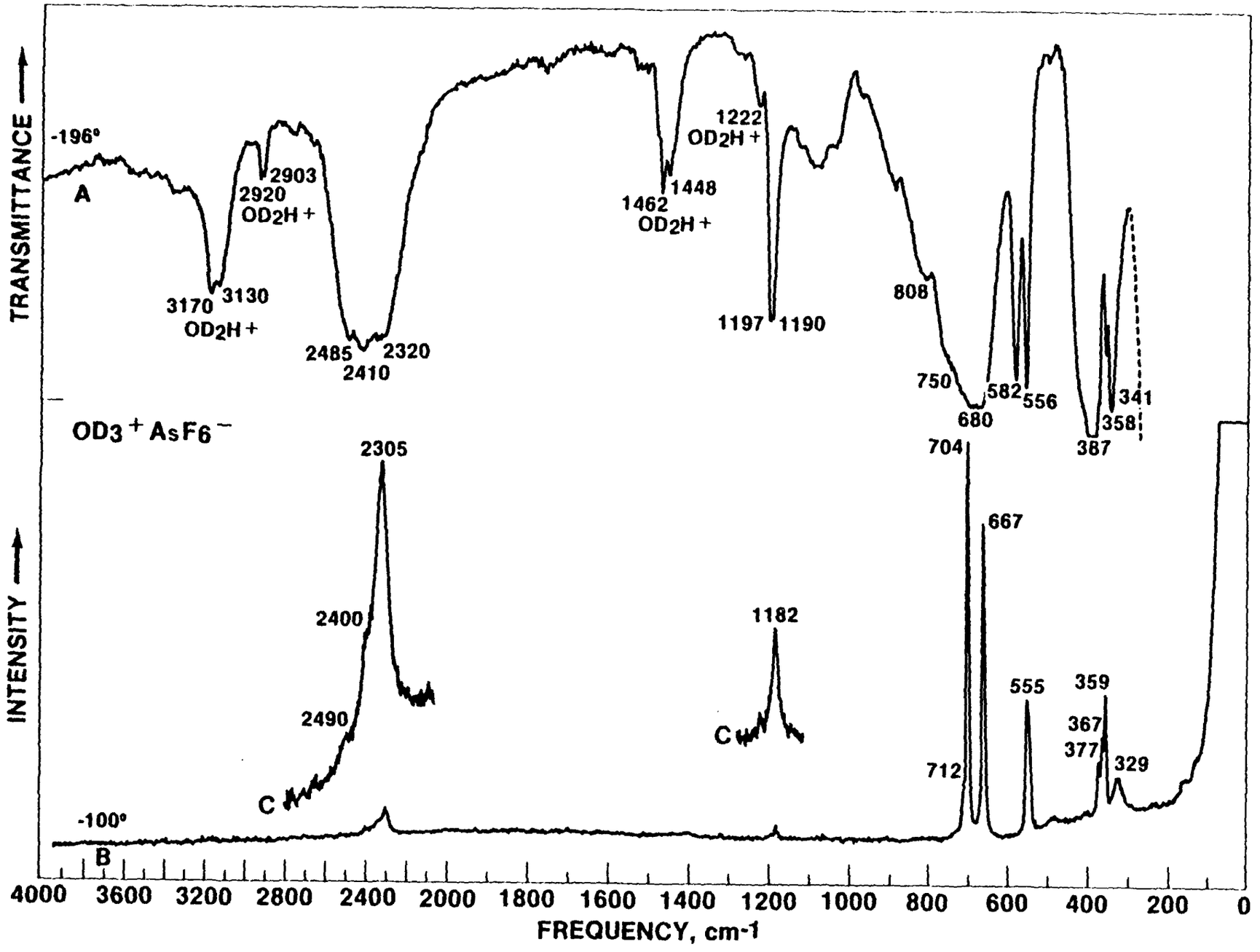
TRANSMITTANCE
-196°
A
3170
3130
OD2H+
2920
2903
OD2H+
2485
2410
2320
1462
1448
OD2H+
1222
OD2H+
1197
1190
808
750
680
582
556
704
387
358
341
OD3+AsF6−
INTENSITY
2305
2400
2490
C
1182
C
712
667
555
359
367
377
329
-100°
B
4000 3600 3200 2800 2400 2000 1800 1600 1400 1200 1000 800 600 400 200 0
FREQUENCY, cm-1

FIGURE 4.

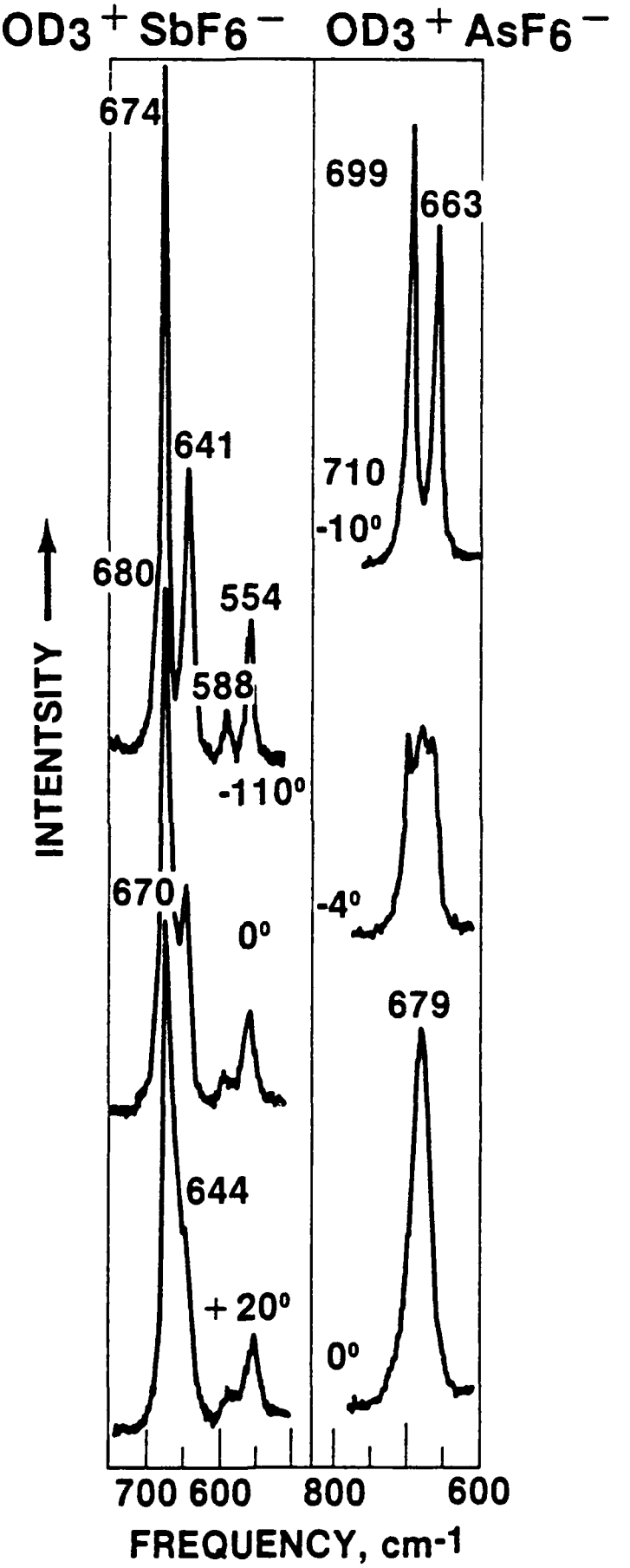
OD3 + SbF6 −
OD3 + AsF6 −
674
641
680
554
588
-110°
670
0°
644
+ 20°
699
663
710
-10°
-4°
679
0°
INTENTSITY
700 600
800 600
FREQUENCY, cm-1

FIGURE 5.

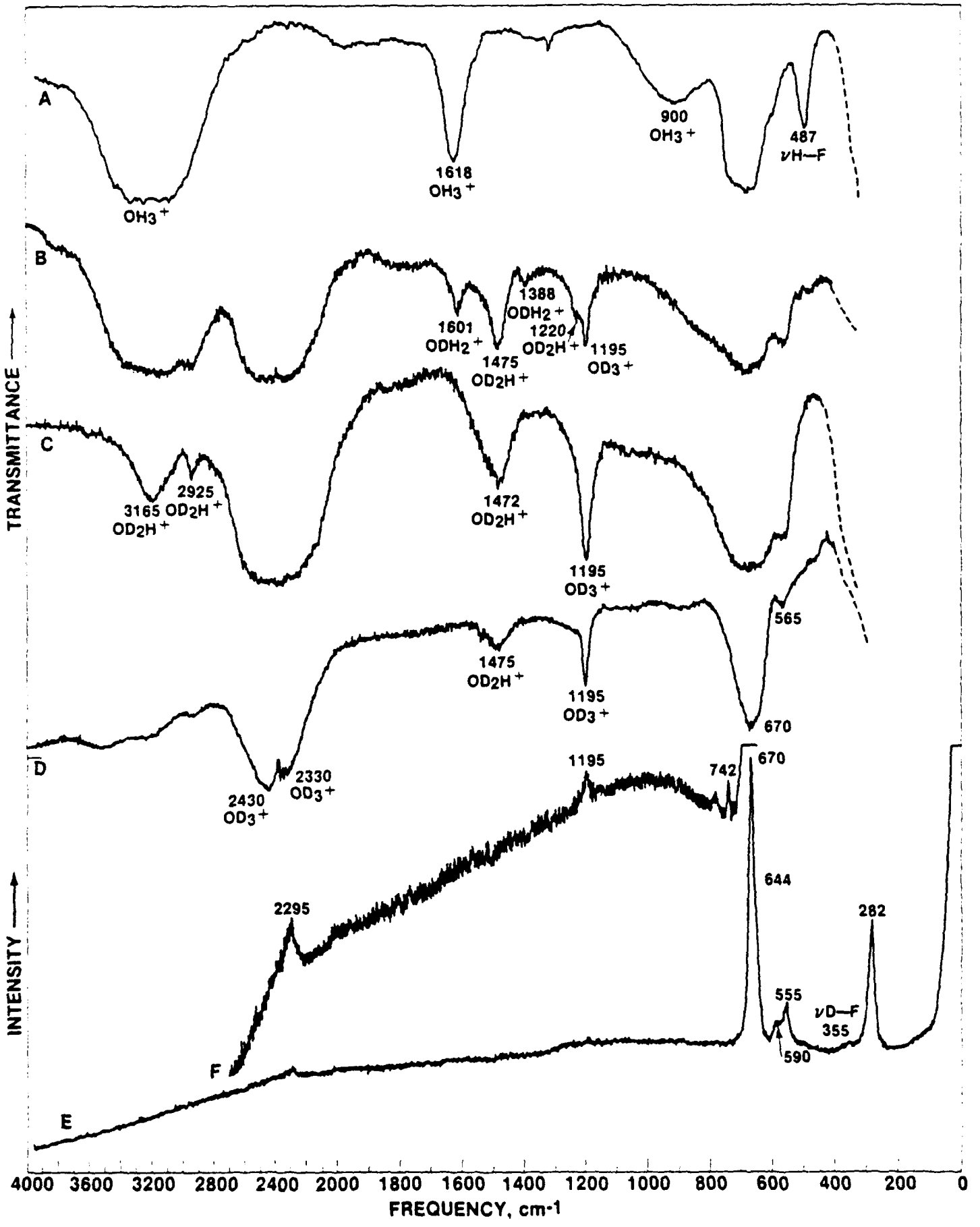
A
OH_3^+
1618
OH_3^+
900
OH_3^+
487
νH—F
B
1601
ODH_2^+
1475
OD_2H^+
1388
ODH_2^+
1220
OD_2H^+
1195
OD_3^+
C
3165
OD_2H^+
2925
OD_2H^+
1472
OD_2H^+
1195
OD_3^+
565
D
2430
OD_3^+
2330
OD_3^+
1475
OD_2H^+
1195
OD_3^+
670
E
F
2295
1195
742
670
644
282
555
νD—F
355
590
TRANSMITTANCE
INTENSITY
4000 3600 3200 2800 2400 2000 1800 1600 1400 1200 1000 800 600 400 200 0
FREQUENCY, cm-1

FIGURE 6.

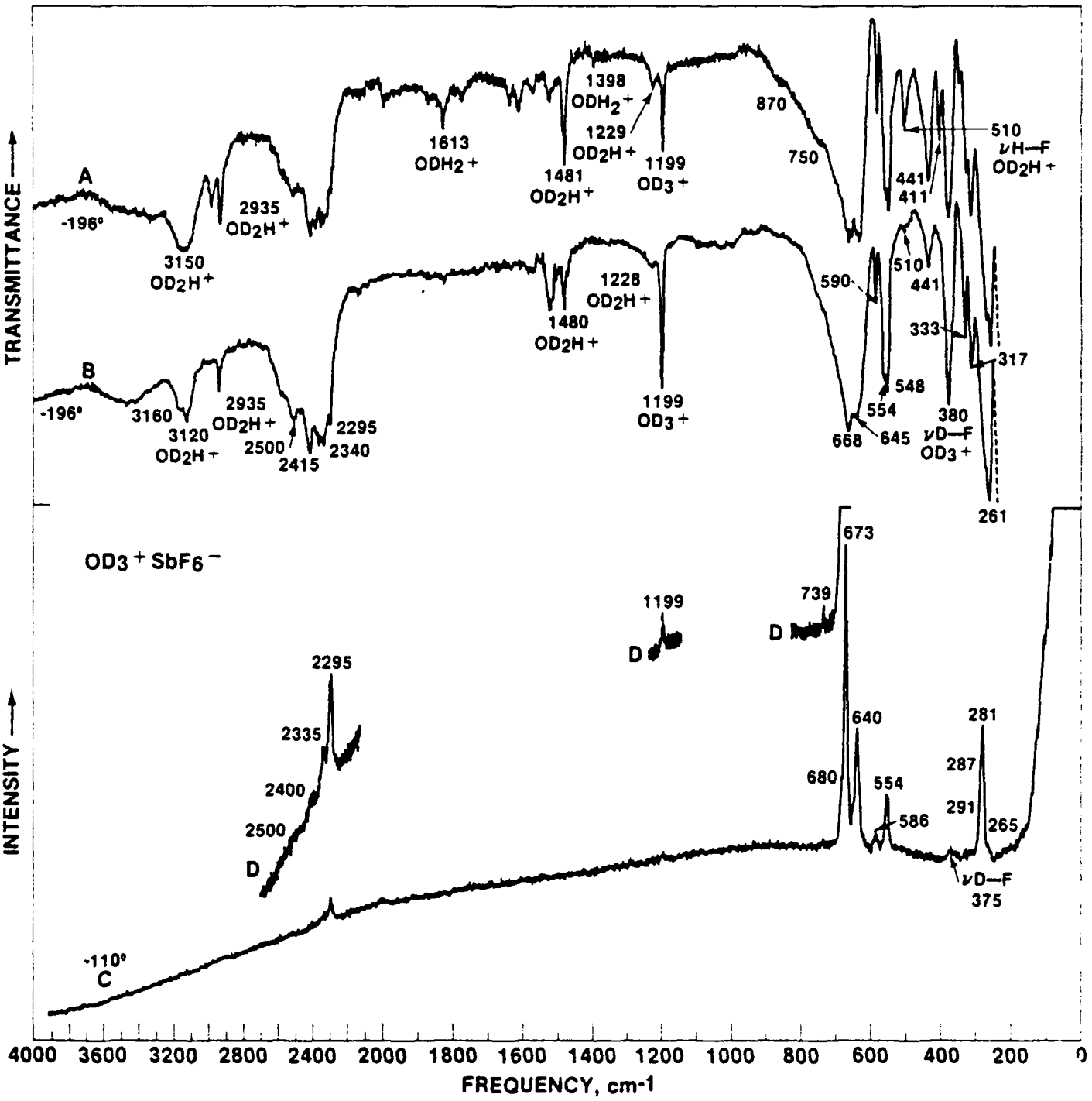
TRANSMITTANCE
A
-196°
3150
OD2H+
2935
OD2H+
1613
ODH2+
1481
OD2H+
1398
ODH2+
1229
OD2H+
1199
OD3+
870
750
510
νH—F
OD2H+
441
411
B
-196°
3160
3120
OD2H+
2935
OD2H+
2500
2415
2295
2340
1480
OD2H+
1228
OD2H+
1199
OD3+
590
668
645
554
548
510
441
380
νD—F
OD3+
333
317
261
OD3+ SbF6−
INTENSITY
1199
D
739
D
673
2295
2335
2400
2500
D
640
680
554
586
281
287
291
265
νD—F
375
-110°
C
4000 3600 3200 2800 2400 2000 1800 1600 1400 1200 1000 800 600 400 200 0
FREQUENCY, cm-1

FIGURE 7.

DL/413/83/01
GEN/413-2

TECHNICAL REPORT DISTRIBUTION LIST, GEN

	No. Copies
Office of Naval Research Attn: Code 413 800 N. Quincy Street Arlington, Virginia 22217	2
ONR Pasadena Detachment Attn: Dr. R. J. Marcus 1030 East Green Street Pasadena, California 91106	1
Commander, Naval Air Systems Command Attn: Code 310C (H. Rosenwasser) Washington, D.C. 20360	1
Naval Civil Engineering Laboratory Attn: Dr. R. W. Drisko Port Hueneme, California 93401	1
Superintendent Chemistry Division, Code 6100 Naval Research Laboratory Washington, D.C. 20375	1
Defense Technical Information Center Building 5, Cameron Station Alexandria, Virginia 22314	12
DTNSRDC Attn: Dr. G. Bosmajian Applied Chemistry Division Annapolis, Maryland 21401	1
Naval Ocean Systems Center Attn: Dr. S. Yamamoto Marine Sciences Division San Diego, California 91232	1
Naval Ocean Systems Center Attn: Technical Library San Diego, California 92152	1
Naval Weapons Center Attn: Dr. A. B. Amster Chemistry Division China Lake, California 93555	1
Scientific Advisor Commandant of the Marine Corps Code RD-1 Washington, D.C. 20380	1
Dean William Tolles Naval Postgraduate School Monterey, California 93940	1
U.S. Army Research Office Attn: CRD-AA-IP P.O. Box 12211 Research Triangle Park, NC 27709	1
Mr. Vincent Schaper DTNSRDC Code 2830 Annapolis, Maryland 21402	1
Mr. John Boyle Materials Branch Naval Ship Engineering Center Philadelphia, Pennsylvania 19112	1
Mr. A. M. Anzalone Administrative Librarian PLASTEC/ARRADCOM Bldg 3401 Dover, New Jersey 07801	1

TECHNICAL REPORT DISTRIBUTION LIST, 053

Dr. M. F. Hawthorne
Department of Chemistry
University of California
Los Angeles, California 90024

Dr. D. Venezky
Chemistry Division
Naval Research Laboratory
Washington, D.C. 20375

Professor O. T. Beachley
Department of Chemistry
State University of New York
Buffalo, New York 14214

Dr. A. Cowley
Department of Chemistry
University of Texas
Austin, Texas 78712

Dr. W. Hatfield
Department of Chemistry
University of North Carolina
Chapel Hill, North Carolina 27514

Professor Richard Eisenberg
Department of Chemistry
University of Rochester
Rochester, New York 14627

Professor K. Niedenzu
Department of Chemistry
University of Kentucky
Lexington, Kentucky 40506

Dr. T. Marks
Department of Chemistry
Northwestern University
Evanston, Illinois 60201

Dr. J. Zuckerman
Department of Chemistry
University of Oklahoma
Norman, Oklahoma 73019

Professor K. M. Nicholas
Department of Chemistry
Boston College
Chestnut Hill, Massachusetts 02167

Professor R. Neilson
Department of Chemistry
Texas Christian University
Fort Worth, Texas 76129

Professor M. Newcomb
Department of Chemistry
Texas A&M University
College Station, Texas 77843

Professor R. Wells
Department of Chemistry
Duke University
Durham, North Carolina 27706